

## Design and Simulation of Archimedes Screw Turbine at Head Below 1 Meter

Naufal Riyandi<sup>1</sup> & Priyono Soetikno<sup>1,2</sup>

<sup>1</sup> Fluid Machinery Laboratory Faculty of Mechanical and Aerospace Engineering,  
Institut Teknologi Bandung, Bandung.

<sup>2</sup> Research Center on New and Renewable Energy, Center for Research and Community  
Services, Institut Teknologi Bandung, Bandung  
Email: naufalriyandi96@gmail.com

**Abstract.** Archimedes Screw Turbine (AST) is an environmentally friendly turbine and can be used at very low heads and small water flowrate which are in accordance with the characteristics of rivers in Indonesia. There is still a lack of research on AST in Indonesia and in order to obtain a theoretical equation to produce turbine performance Therefore, this study was conducted to design the AST, determine the theoretical equation for calculating AST performance, determine the optimum water flowrate, and analyze the characteristics of the AST against variations in the rotational speed of each flights, inclination angle, and optimum flowrate water. This research produces AST with one flight and two flights with optimum dimension. The theoretical equation has been formulated by producing an error from 8% to 0.4%. The optimum water flowrate in the AST for 1 flight is 4l/s, while for 2 flights is 8l/s. The maximum torque for 1 flight is 1.03Nm and for 2 flights is 2.14Nm with optimum rotational speed and an inclination angle are 14.7rad/s 29°. The maximum turbine power for 1 flight is 15.14W and for 2 flights is 31.46W with optimum rotational speed and inclination angle are 14.7 rad/s 29°. The maximum turbine efficiency for 1 flight is 80.70% and 2 flights is 82.68% with optimum rotational speed is 14.7rad/s and optimum inclination angle for 1 flight is 27° while 2 flights is 29°.

**Keywords:** *AST, Low Head, Performance, Small Flowrate, Theoretical Equation.*

### 1 Introduction

The higher emission of greenhouse gases, one of which is CO<sub>2</sub>, makes the earth's temperature higher, which is a factor causing the climate crisis [1][2]. One of the efforts to reduce the climate crisis is to develop clean energy and increase the use of renewable energy [3]. One of the countries that can contribute a large use of renewable energy is Indonesia. Indonesia has a renewable energy potential of 442 GW with water energy as the largest renewable energy potential, which is worth 94.3 GW [4]. However, the use of renewable energy, especially water energy in Indonesia is still relatively low, with an installed capacity of 5,969.15 MW in 2019 [5].

One of the reasons for the low utilization of water energy potential in Indonesia is environmental factors. The construction of large-scale hydroelectric power plants can endanger fish and aquatic biota, both from water structures and from turbine flights [6]. Therefore, to maximize the potential of water while considering environmental aspects, micro and pico hydroelectric power plants can be used using environmentally friendly turbine types. One type of turbine that can be used is the Archimedes Screw Turbine (AST).

AST is a turbine that is more environmentally friendly, especially for aquatic biota such as fish. In addition, the use of AST is also very suitable and efficient at very low heads with small discharges, which are in the range of 60-80% [7]. Thus, the use of AST as a turbine to utilize water energy in Indonesia is very suitable because of Indonesia has many rivers with low head, so that the potential for water utilization can be more optimal [8]. Several studies have been carried out related to AST. In Edirisinghe's (2021) study, a simulation was conducted to determine the efficiency of AST if it is at a high inclination angle, which is 450. The research resulted that the AST with an inner diameter of 0.643 m and an outer diameter of 1.2 m, 3 flights, an inclination angle of 450 and a flow rate of 0.232 m<sup>3</sup>/s, was able to produce an efficiency of around 82%. When the angle is increased, with the same diameter and flow rate, the efficiency is below 82% but is still in the range of 80% [9]. Another research was conducted by Dellinger who examined the effect of inclination and number of flights on AST in 2019. From the results of his research, it was found that in AST with 4 and 5 flights, it was found that the highest efficiency was in the angle range of 200 - 25.40. Meanwhile, for the number of 3 flights, the highest efficiency is at an angle of about 15.50 [10]. The optimization of the AST design has also been studied by Shahverdi in 2020. With this optimization design, the highest efficiency that can be achieved by the AST with a geometry of 6 m long, number of flight 1, and an inclination of 200 is 90.83% [11].

Although there have been several studies on AST, research and utilization of AST in Indonesia is still rare [12]. Therefore, in this study, the design and simulation of AST at a head below 1 m with variations of flights 1 and 2, variations in flow rate of 4 l/s, 5 l/s, and 6 l/s, variations inclination 200 220, 250, 270, and 290 will be carried out in this study, as well as variations in rotational speed of 5 rad/s, 10 rad/s, 12 rad/s, 14.7 rad/s, 17 rad/s and 20 rad/s. These variations were carried out in order to obtain the characteristics of the AST power to variations in the angle of inclination, the torque characteristics of the AST to variations in rotational speed, and to know the maximum power of the AST design. The research was carried out theoretically by combining several existing equations and then being tested by computational simulations.

## 2 Methodology

There are three major methods in this research. The first is to calculate geometry design the AST, the second is to calculate the power and efficiency of designed AST theoretically, the third is to simulate the designed AST with Computational Fluid Dynamic Simulation for comparing between simulation and theoretical results.

### 2.1 Geometry Design

In designing the geometry of AST, several mathematical equations were used to determine the dimensions which had previously been formulated by Rorres in [13]. In this research, the internal diameter assumed to be equal to 0.104 m or 4 inch, based on pipe diameter that common available, and the length of the AST assumed to be constant along 1 m, to make them easier to carried on.

$$R_i = \rho^* R_o \quad (1)$$

$$L = \frac{H}{\sin \theta} \quad (2)$$

$$K = \tan \theta \quad (3)$$

$$(4a)$$

$$\Lambda = 2,4R_o \text{ if } \theta < 30^\circ$$

$$\Lambda = 2,0R_o \text{ if } \theta = 30^\circ \quad (4b)$$

$$\Lambda = 1,6R_o \text{ if } \theta > 30^\circ \quad (4c)$$

$$G_w = 0,0045\sqrt{D_o} \quad (5)$$

$$m = \frac{L}{\Lambda} \quad (6)$$

$$V_T = \pi R_o^2 \Lambda v^* m \quad (7)$$

$$n = \frac{50}{(2R_o)^{2/3}} \quad (8)$$

The value of  $\rho^*$  and  $v^*$  is influenced by the number of flights to be designed. To find out the value of  $\rho^*$  and  $v^*$ , it can be seen in Figure 1 [13]. From the calculation results, the AST design is obtained for the number of flights 1 and 2 with the values in table 1.

Number of blades $N$ (1)	Optimal radius ratio $\rho^*$ (2)	Optimal pitch ratio $\lambda^*$ (3)	Optimal volume-per- turn ratio $\lambda^*v(N, \rho^*, \lambda^*)$ (4)	Optimal volume ratio $v(N, \rho^*, \lambda^*)$ (5)
1	0.5358	0.1285	0.0361	0.2811
2	0.5369	0.1863	0.0512	0.2747
3	0.5357	0.2217	0.0598	0.2697
4	0.5353	0.2456	0.0655	0.2667
5	0.5352	0.2630	0.0696	0.2647
6	0.5353	0.2763	0.0727	0.2631
7	0.5354	0.2869	0.0752	0.2619
8	0.5354	0.2957	0.0771	0.2609
9	0.5356	0.3029	0.0788	0.2601
10	0.5356	0.3092	0.0802	0.2592
11	0.5358	0.3145	0.0813	0.2586
12	0.5360	0.3193	0.0824	0.2580
13	0.5360	0.3234	0.0833	0.2574
14	0.5360	0.3270	0.0841	0.2571
15	0.5364	0.3303	0.0848	0.2567
16	0.5362	0.3333	0.0854	0.2562
17	0.5362	0.3364	0.0860	0.2556
18	0.5368	0.3380	0.0865	0.2559
19	0.5364	0.3404	0.0870	0.2555
20	0.5365	0.3426	0.0874	0.2551
21	0.5370	0.3440	0.0878	0.2553
22	0.5365	0.3465	0.0882	0.2544
23	0.5369	0.3481	0.0885	0.2543
24	0.5367	0.3500	0.0888	0.2538
25	0.5371	0.3507	0.0891	0.2542
.	.	.	.	.
.	.	.	.	.
.	.	.	.	.
$\infty$	0.5394	0.3953	0.0977	0.2471

**Figure 1** Optimal Parameter Ratio for AST Design based on Variation in Number of Blades.

**Table 1** Parameters of AST.

Parameters	Flights	
	1	2
Inner Diameter (m)	0.104	
Outer Diameter (m)	0.214	0.212
Pitch (m)	0.26	
Gap Width (m)	0.002078	0.002076
m	4	

## 2.2 Theoretical Calculation

In this study, before the computational fluid dynamic simulation is run, theoretical calculations were carried out to obtain the power and efficiency of the AST design. The equation used in this calculation is to use the equation that was previously done by Müller in [15] and combining with equation from Shahverdi in [11] to get more precision result. For the hydraulic force and hydraulic power, equation from Müller is used.

$$Q = A_E v_1 \quad (9)$$

$$v_1 = \frac{Q}{A_E} \quad (10)$$

$$A_E = \frac{\pi D_o^2}{4} \quad (11)$$

$$P_{teori} = F_{hyd} v_1 \quad (12)$$

$$F_{hyd} = \frac{(d_0 + \Delta d)^2 - d_0^2}{2} \rho g \quad (13)$$

$$\Delta d = \Lambda \tan \theta \quad (14)$$

To determine the initial water level ( $d_0$ ), substituted from the equation that has been developed and optimized by Shahverdi in [11].

$$d_0 = z_{min} + f(z_{max} - z_{min}) \quad (15)$$

$$z_{min} = -\frac{D_o}{2} \cos \theta - \frac{\Lambda}{2} \sin \theta \quad (16)$$

$$z_{max} = \frac{D_o}{2} \cos \theta - \frac{\Lambda}{2} \sin \theta \quad (17)$$

The value of  $f$  is the water fill factor in the AST. When  $f = 0$ , then no water flows through the AST [11].

### 2.3 Computational Simulation

After theoretical calculations, computational analysis is carried out. The output of this computational simulation is in the form of torque, which torque will be used to determine the amount of AST power computationally. To determine the amount of power generated by the AST, the following equation can be used.

$$P_{AST} = \tau \omega \quad (18)$$

$$\omega = \frac{2\pi n}{60} \quad (19)$$

Thus, the efficiency produced by AST can be known by the following equation (20). Meanwhile, to determine the efficiency of the theoretical power of AST, it can be seen from the following equation.

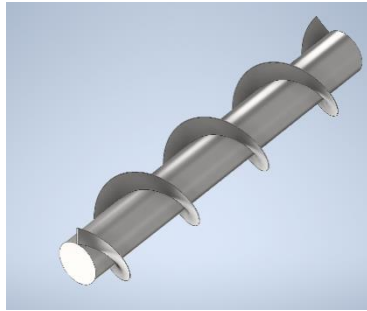
$$\eta = \frac{P_{AST}}{P_{avail}} \quad (20)$$

$$\eta = \frac{P_{teori}}{P_{avail}} \quad (21)$$

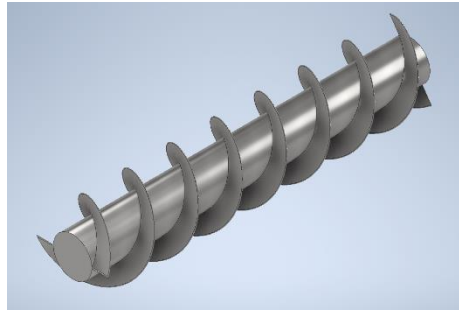
Before the simulation is run, the design modelling is carried out first as shown in Figure 2 and Figure 3. The setting of the computational simulation can be seen in

Figure 4. Because the turbine rotation axis is not on the global axis, but on the tilt axis, to determine the turbine torque can use the following trigonometric approach.

$$\tau = \frac{\tau}{\sin \theta} \quad (22)$$



**Figure 2** AST N=1



**Figure 3** AST N=2

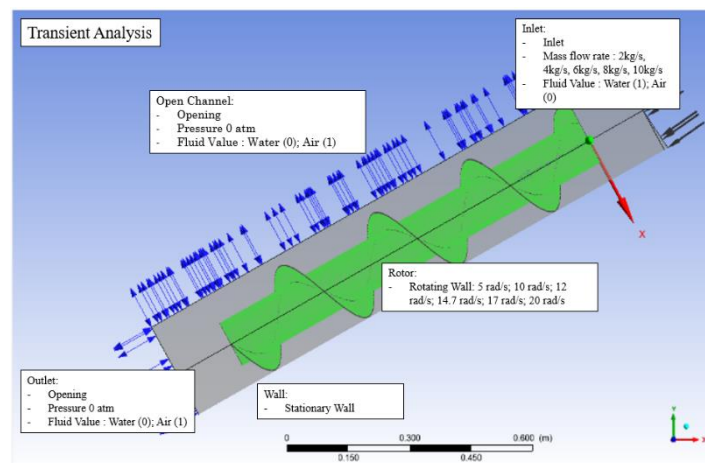


**Figure 4** Simulation Setting.

### 3 Results

#### 3.1 Validation of Simulation

Validation is done by performing numerical simulations using predetermined settings for laboratory-scale experimental research. In the validation for this

thesis research, the model from Erinofiardi in [16] is used with the following parameters.

The torque that can be generated by the AST turbine is 0.0030 Nm on the global y-axis. Therefore, on the AST rotation axis, with an inclination angle of 450, the result is 0.0042 Nm. Thus, the power that can be generated by the AST is 0.092 W. Meanwhile, the laboratory test results are 0.098 W. This results in an error of 5.1% in the simulation. This error occurs because the simulation does not take into account the losses that arise in the actual situation, such as losses due to bearings, losses to outlets, and losses to flowrates.

**Table 2** Erinofiardi AST Parameters for Validation.

<b>Diameter (m)</b>	<b>0,106</b>	
<b>Pitch (m)</b>	0,08	
<b>Length (m)</b>	0,7	
<b>Flowrate (l/s)</b>	0,68	
<b>Water Velocity (m/s)</b>	0,0041	
<b>Flighht</b>	1	
<b>Rotational Speed (RPM)</b>	232	946
<b>Inclination Angle (°)</b>	45	
<b>Power (W)</b>	0,098 W	0,2772 W

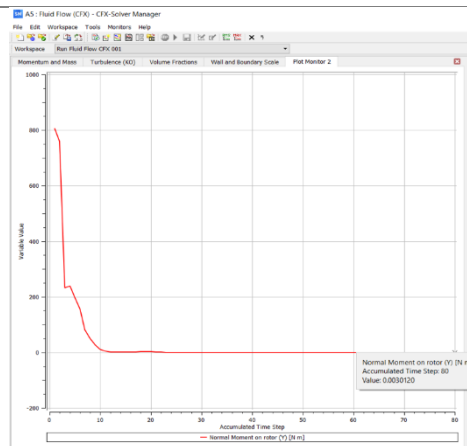


**Figure 5** AST Validation Torque on Global Y Axis.

### 3.2 Theoretical Results

The calculation results show that the greater the discharge flowing in the AST, the greater the power that the AST can produce as shown in Figure 6. This is in accordance with the theory which states that the power and flow rate are directly proportional. In addition, when compared to the power generated against variations in the angle of inclination, 200, 220, 250, 270, and 290, it shows that the greater the angle, the greater the power generated. This is because, in this study, the value of  $L$  or the length of the AST is kept constant at 1m, so that when there is a change in the angle of inclination, there is also a change in the height of the water fall or the head used. The relationship between the angle of inclination and the head is directly proportional. So, the bigger the angle, the higher the head. The higher the head, the greater the power that can be generated. This is in accordance with the theory which states that power and head are directly proportional.

The power produced is also influenced by changes in the number of flights used. In this study, two variations of the number of flights were used, namely  $N=1$  and  $N=2$ . The results of theoretical calculations show that the more the number of flights, the greater the power that can be generated by the AST. This is because, the more the number of flights, the more volume of water that can be filled. The larger the volume of water that is accommodated, the greater the power that the AST can produce. This is in accordance with the theory which states that the volume is directly proportional to the water discharge, while the water discharge is directly proportional to the power that can be generated.

Meanwhile, at the results of the calculation of the power that can be produced with potential power, the efficiency values are in the range of 78% to 84%. The highest efficiency is found at the inclination angle of 290 which is 83.68% for  $N=1$  and 83.87% for  $N=2$ . These results indicate that the calculation results are in accordance with the theory because the efficiency range in AST is 60% to 80% [7].

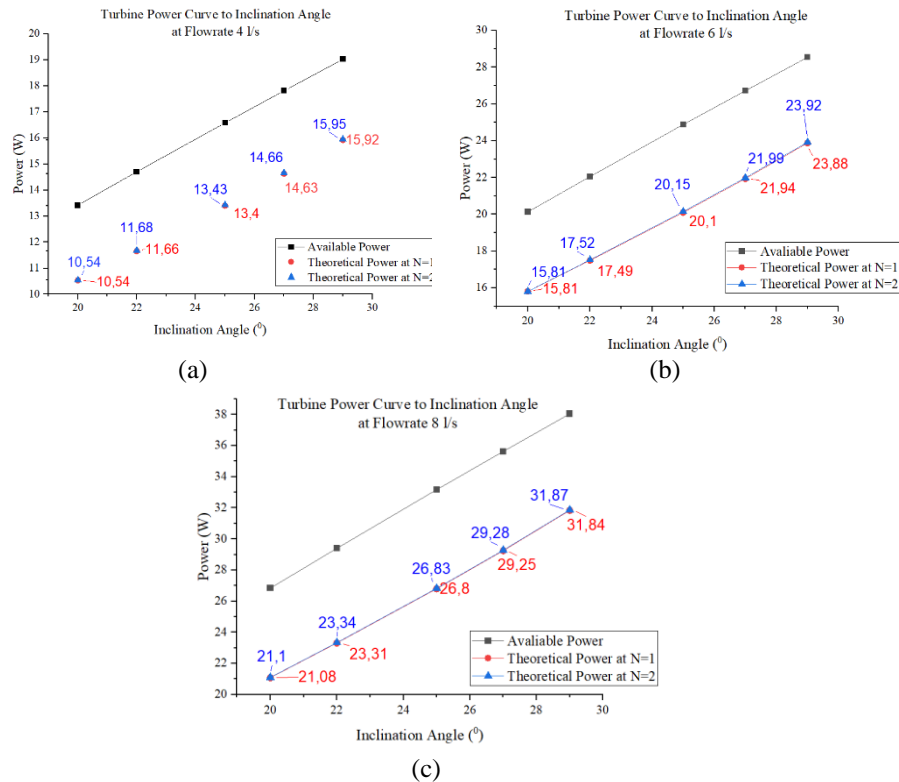


**Figure 6** Curve of Turbine Power to Variation of Inclination Angle at Flowrate: (a) 4 l/s; (b) 6 l/s; (c) 8 l/s

### 3.3 Computational Simulation Results

#### 3.3.1 Turbine Characteristics of Water Flowrate

On the characteristics of the AST turbine to flowrate, the simulation was carried out at a rotational speed of 14.7 rad/s. The rotational speed is chosen based on theoretical calculations for the turbine dimensions that have been designed. The inclination angle chosen is 290 because theoretically, this angle has higher efficiency and power than other angles in the variations used. Simulations were carried out at a discharge range of 2 l/s to 8 l/s for 1 turbine flight, and a discharge range of 4 l/s to 10 l/s for 2 turbine flights. Based on the simulation results, the AST turbine power curve against flow rate and efficiency curve of AST turbine to flow power.

In Figure 7, namely the effect of turbine power on water flowrate, it can be seen that the greater the flowrate that flows, the greater the power that can be

generated. At a flowrate of 8 l/s, the power that can be generated by the turbine is 15.4 Watt. This is in accordance with the theory of hydraulic power which states that the relationship between power and discharge is proportional or directly proportional. Meanwhile, in Figure 8, which is the effect of efficiency on flowrate, it can be seen that the parabolic curve has a peak efficiency, which is at 4 l/s flow rate of 80.97%. Starting from the discharge of 6 l/s, there is a decrease in efficiency due to water in the AST experiencing overflow as shown as Figure 10.

In Figure 11, the influence of turbine power on the flow rate for turbine flights 2, the same as in turbine flight equal to 1, it can be seen that the greater the flow of flowing water, the greater the power that the turbine can produce. This shows that the flowrate is proportional to the power generated by the turbine. In Figure 11, the greatest power is at 10 l/s water discharge, which is 35.2 Watt. In Figure 12, namely the effect of efficiency on the flow of water for a turbine with 2 flights, there is a maximum point on the curve that shows the maximum efficiency that can be achieved by the turbine. In Figure, the highest efficiency is 81.13% with a flow rate of 8 l/s. The same thing happened to turbine flights equal to 2, namely efficiency decreased when overflow occurred. Overflow occurs when the flow rate is increased from 8 l/s to 10 l/s as shown as Figure 14.

The difference in flow rate that causes the overflow phenomenon in turbine flights one and two shows that there are differences in the volume of water that can be accommodated by the turbine. The more turbine flights in the turbine, the greater the volume of water that can be accommodated. The greater the volume of water that can be accommodated, the greater the discharge that can flow in the turbine. Thus, the more the number of flights in the AST, the greater the flow rate that can flow.

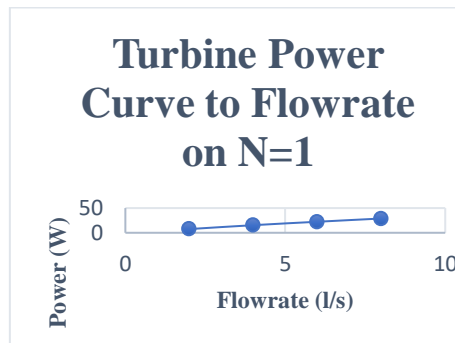


**Figure 7** Turbine Power Curve to Flowrate on N=1

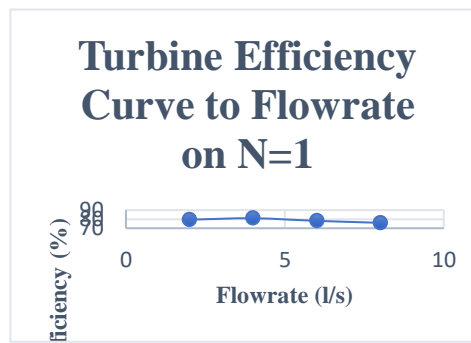


**Figure 8** Turbine Efficiency Curve to Flowrate on N=1

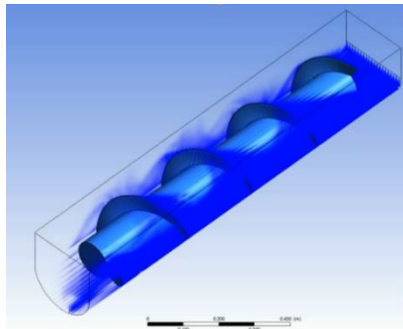


**Figure 9** Flow at Water Flowrate 4 l/s on N=1

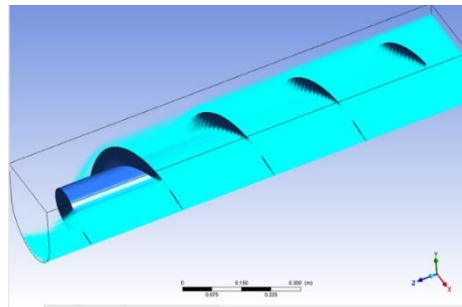


**Figure 10** Flow at Water Flowrate 6 l/s on N=1

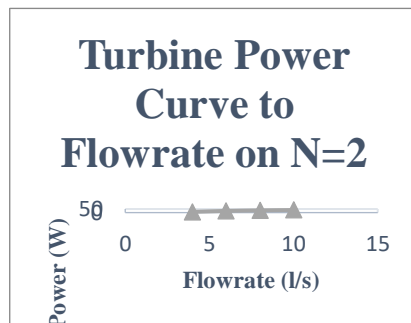


**Figure 11** Turbine Power Curve to Flowrate on N=2

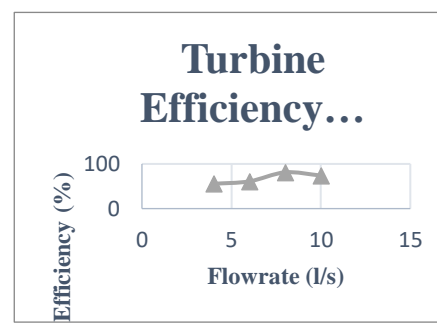


**Figure 12** Turbine Efficiency Curve to Flowrate on N=2

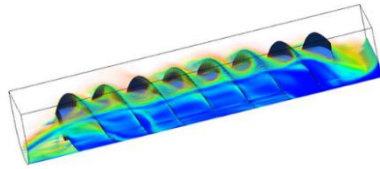


**Figure 13** Flow at Water  
Flowrate 8 l/s on N=2

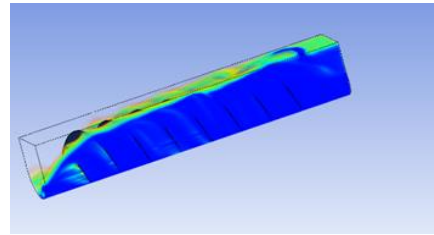


**Figure 14** Flow at Water Flowrate  
10 l/s on N=2

### 3.3.2 Turbine Torque Curve to Rotational Speed

In the simulation results of turbine flights 1 and 2, the simulation is carried out by varying the inclination angle and each angle is simulated by varying the rotational speed. From the simulation results, the results show that in both turbine flights 1 and 2, the rotational speed that produces maximum torque is 14.7 rad/s. The torque value is increasing from 5 rad/s to 14.7 rad/s and after 14.7 rad/s, the torque value is decreasing. This shows that at a rotational speed of 14.7 rad/s, the volume of water that fills the bucket from the turbine is optimum so that the hydrostatic force that causes the turbine to rotate is optimal.

At one flight turbine, the torque at a rotational speed of 14.7 rad/s for an inclination angle of 200 is 0.66 Nm, at an angle of 220 is 0.78 Nm, at an angle of 250 it is 0.89 Nm, at an angle of 270 is equal to 0.980, and at an angle of 290 the torque produced is 1.03 Nm. Meanwhile, at turbine flights 2, the torque produced by the turbine at a rotational speed of 14.7 rad/s for an inclination angle of 200 is 1.41 Nm, at an angle of 220 is 1.58 Nm, at an angle of 250 is 1.80 Nm, at an angle of 270 is 1.94 and the torque at an angle of 290 is 2.14 Nm. These torque values indicate that the amount of torque is influenced by the angle and also the head of the turbine. In this study, the greater the angle of inclination which also means that the higher the head, the greater the torque that can be generated. In addition, the torque produced by turbine flights 2 is greater than turbine flight 1. This is because the more flights, the greater the turbine's ability to rotate. This is because, the hydrostatic force generated by the water moves each flights in the AST.

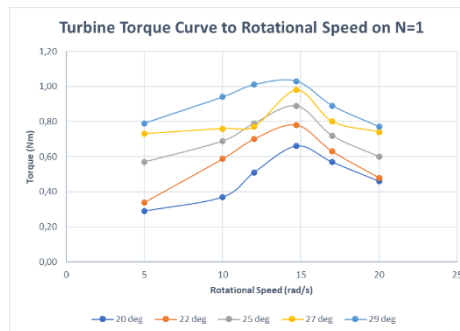


**Figure 15** Turbine Torque Curve to Rotational Speed on N=1

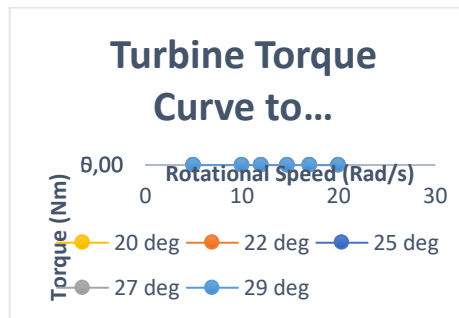


**Figure 16** Turbine Torque Curve to Rotational Speed on N=2

### 3.3.3 Turbine Power Curve to Rotational Speed

Power is the function of torque and rotational speed. Therefore, the amount of power that can be generated by the turbine in this study, both at one and two turbine flights, is strongly influenced by the amount of torque and also the rotational speed of the turbine. Thus, on turbine power, both one and two turbine flights, there is an optimum point where the power generated by the turbine is maximum. In both turbine flight one and turbine flights 2, the optimum power is obtained at an angular velocity of 14.7 rad/s. As with torque, after passing 14.7 rad/s, the power decreases because the water that fills the bucket in the turbine is also not optimal.

At one turbine flight, with a rotational speed of 14.7 rad/s, the power that can be generated by the turbine at an inclination angle of 200 is 9.71 Watt, then at an angle of 220 it is 11.44 Watt, at an angle of 250 it is worth 13.06 Watt, at the inclination 270 worth 14.38 Watt, and then the power that can be generated at the inclination of the turbine 290 is 15.14 Watt. Meanwhile, in turbine flights two, the power that can be produced is greater than in turbine flight 1. This is the same as torque, the more flights will have implications for the greater the torque and cause the greater the power that can be generated by the AST.

At the turbine flights two, using a rotational speed of 14.7 rad/s, the power that can be generated by the AST for a turbine inclination of 200 is 20.73 Watt, then at inclination of 220 it is 23.23 Watt, at a turbine inclination 250 is worth 26.44 Watt, then at an inclination angle of 270 it is 28.52 Watt, and at a turbine inclination of 290 the power that can be produced by the turbine increases to 31.46 Watt.

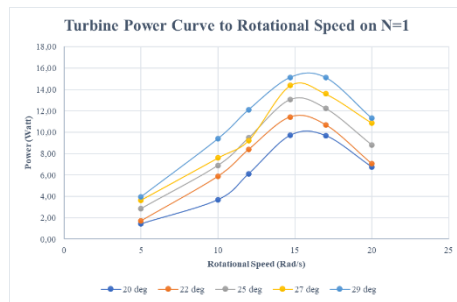


**Figure 17** Turbine Power Curve to Rotational Speed on N=1

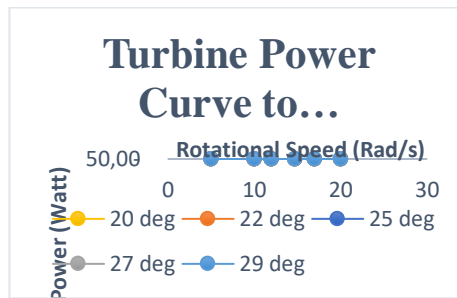


**Figure 18** Turbine Power Curve to Rotational Speed on N=2

### 3.3.4 Turbine Efficiency Curve to Rotational Speed

The amount of efficiency is obtained from the results of the division between the simulated power and the available power based on the head and water flow rate. The greater the power simulation results approach the amount of available power, the higher the efficiency value obtained. In this study, as with torque and power, there is a maximum point on the efficiency curve which indicates that there is an optimum efficiency in the designed AST. Maximum efficiency is also obtained at a rotating speed of 14.7 rad/s.

In one turbine blade, the maximum efficiency that can be achieved is from the range of 70% to 81%. At an inclination angle of 200, the maximum efficiency that can be achieved is 72.36%, at an angle of 220 it is 77.84%, at an angle of 250 the AST efficiency is 78.73%, at an angle of 270 the efficiency reaches a maximum point of 80.70%, and at an angle of 290 the efficiency decreases to 79.59%. In turbine blade two, the maximum efficiency that can be achieved is greater than turbine blade one, which is from the range of 77% to 83%. The efficiency of the AST simulation at a turbine tilt angle of 200 is 77.22%, at an angle of 220 it is worth 79%, at an angle of 250 it is worth 79.70%, at an angle of 270 is worth 80.04%, and at an angle of 290 it reaches a maximum efficiency of 82.68%.

The difference between the simulation results and the available power is caused by several things, including, in the simulation, taking into account the effect of viscosity, wall function, turbulence, and the influence of angle. While the available power only takes into account the flow rate and head without an estimate of the inclination angle so that the height is only considered perpendicular to the surface (free fall motion). In the calculation of available power, the effect of viscous and wall function is also not taken into account. The optimum results from the simulations for the AST design can be summarized in table 3.

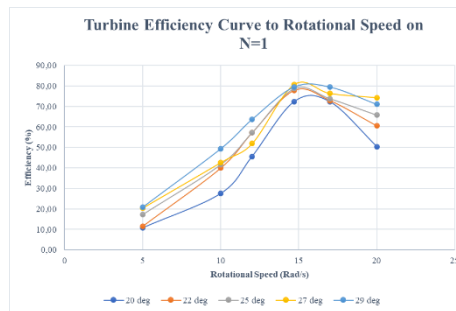


**Figure 19** Turbine Efficiency Curve to Rotational Speed on N=1

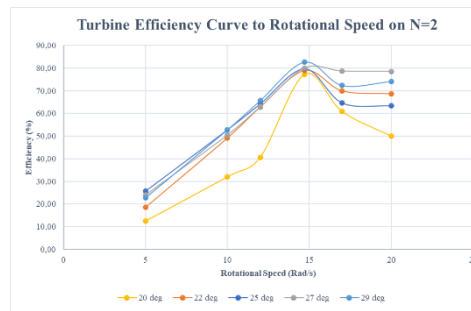


**Figure 20** Turbine Efficiency Curve on Rotational Speed on N=2

**Table 3** Optimum Results of AST Computational Simulation.

	Flight 1	Flights 2
Max Flowrate (l/s)	4	8
Max Power (Watt)	15.14	31.46
Max Torque (Nm)	1.03	2.14
Max Efficiency (%)	80.70	82.68
Max Inclination ( $^{\circ}$ )	29	29
Efficient Inclination ( $^{\circ}$ )	27	29

### 3.4 Comparison between Theoretical and Simulation Results

The results of the calculation of the theoretical AST power and the maximum power from the simulation results can be seen in table 4. As shown in table 4, the AST simulation results, which represent the real situation, have a maximum power result that is relatively similar to the theoretical calculated power. This can be seen from the resulting error value in the range of 8% to 0.4%. The error value is because the theoretical calculation does not take into account the effect of viscosity and turbulence effect.

**Table 4** Comparison between Turbine Power by Theoretical Equation and Simulation

N=1					
	Power				
	Inclination Angle (°)				
	20	22	25	27	29
<b>Theoretical</b>	10.54 W	11.68 W	13.43 W	14.66 W	15.95 W
<b>Simulation</b>	9.71 W	11.44 W	13.06 W	14.38 W	15.14 W
<b>Error</b>	7.86%	1.84%	2.57%	1.71%	4.89%
N=2					
	Power				
	Inclination Angle (°)				
	20	22	25	27	29
<b>Theoretical</b>	21,10 W	23,39 W	26,89 W	29,35 W	31,94 W
<b>Simulation</b>	20,73 W	23,23 W	26,44 W	28,52 W	31,46 W
<b>Error</b>	1,77%	0,48%	1,47%	2,61%	1,29%

#### 4 Conclusions

Based on the research that has been done, it can be concluded that:

1. The Archimedes Screw Turbine is designed with two variations of blades, namely flight 1 and flights 2. In flight 1, the AST has an outer radius of 0.107 m, an inner radius of 0.057 m, a pitch of 0.26 m, the distance between the flight and the waterway is 0.002076 m, the number of threads is 4. While in the flights 2, the AST has an outer radius of 0.106, an inner radius of 0.057 m, a pitch of 0.26 m, the distance between the flights and the waterway is 0.002079 m, and the number of threads is 4.
2. Theoretical equations have been formulated by producing errors obtained from comparing the theoretical calculation results and simulation results ranging from 8% to 0.4%.
3. The optimum water discharge that can flow in the AST for the number of flight 1 is 4 l/s, while for the number of flights 2 is 8 l/s.
4. The torque characteristics of the AST are shown in Figures and with the maximum torque for flight 1 worth 1.03 Nm and for flights 2 worth 2.14 Nm which is at the optimum point, namely at a rotational speed of 14.7 rad. /s and the angle of inclination is 29°.

5. The power characteristics of the AST are shown in Figures and with a maximum turbine power value for flight 1 of 15.14 W and for flights 2 of 31.46 W which is at the optimum point, namely at a rotational speed of 14, 7 rad/s and an inclination angle of  $29^0$ .
6. The efficiency characteristics of the AST are shown in Figures and with the maximum turbine efficiency value for flight 1 of 80.70% which is located at the optimum point at an inclination angle of  $27^0$  and a rotational speed of 14.7 rad/s. While on turbine flights 2, the maximum efficiency is 82.68% which is located at the optimum point at the inclination angle of  $29^0$  with a rotational speed of 14.7 rad/s.

List the nomenclature in alphabetical order. List Roman letters followed by Greek symbols followed by subscript and superscripts.

$A$	=	Amplitude
$C_d$	=	drag coefficient
$f_e$	=	linearization coefficient
$K_i$	=	modification factor
$\gamma$	=	wave number
$\psi$	=	Complex wave number

## 5 Nomenclature

$\Lambda$	Pitch (m)
$\Delta d$	Increasing of Water Depth (m)
$\pi$	Constant
$\eta$	Efficiency (%)
$\rho$	Density ( $\text{kg/m}^3$ )
$\rho^*$	Optimum radius ratio
$\tau$	Torque (Nm)
$\theta$	Inclination Angle ( $^0$ )
$\omega$	Rotational Speed (Rad/s)
$A_E$	AST Cross-Section ( $\text{m}^2$ )
$D_0$	Outer Diameter (m)
$d_0$	Initial Height of Water Entering Turbine (m)

$f$	<i>Fill Factor</i>
$F_{hyd}$	Hydraulic Force of AST (N)
$g$	Gravity (m/s <sup>2</sup> )
$G_w$	Gap Width between Flights and Waterway (m)
$H$	Head (m)
$L$	Lenght (m)
$m$	Threads (m)
$n$	RPM
$P_{AST}$	Simlation Power of AST (W)
$P_{avail}$	Available Power of AST (W)
$P_{teori}$	Theoretical Power of AST (W)
$Q$	Water Flowrate (m <sup>3</sup> /s)
$R_i$	Inner Radius (m)
$R_o$	Outer Radius (m)
$v^*$	Optimum Volume Ratio
$v_1$	AST Velocity (m/s)
$V_T$	Volume Bucket (m <sup>3</sup> )
$z_{max}$	Height Above Water Level (m)
$z_{min}$	Height Below Water Level (m)

## References

- [1] R. Pratama, *Efek rumah kaca terhadap Bumi, Tanaman, dan Atmosfer*, Efek rumah kaca (Green House Eff. ), **3814**, no. Green House Effect, pp. 120–126, 2019.
- [2] EPA, *Higher Temperatures | A Student's Guide to Global Climate Change* / US EPA," 2017. <https://archive.epa.gov/climatechange/kids/impacts/signs/temperature.html> (22 June 2021).

- [3] Kementerian Lingkungan Hidup dan Kehutanan Republik Indonesia, *First Nationally Determined Contribution Republic of Indonesia*, 2016. [Online]. Available: [https://www4.unfccc.int/sites/ndcstaging/PublishedDocuments/Indonesia First/First NDC Indonesia\\_submitted to UNFCCC Set\\_November 2016.pdf](https://www4.unfccc.int/sites/ndcstaging/PublishedDocuments/Indonesia%20First/First%20NDC%20Indonesia_submitted%20to%20UNFCCC%20Set_November%202016.pdf).
- [4] Dewan Energi Nasional, *Outlook Energi Indonesia 2019*, no. ISSN 2527 3000, 2019.
- [5] KESDM, *Rencana Strategis Direktorat Jenderal Energi Baru, Terbarukan dan Konservasi Energi 2020-2024*. Jakarta: Direktorat Jenderal Energi Baru, Terbarukan dan Konservasi Energi, 2020.
- [6] Erinofiardi,., *A Review on Micro Hydropower in Indonesia*,” *Energy Procedia*, **110**, no. March, pp. 316–321, 2017, doi: 10.1016/j.egypro.2017.03.146.
- [7] A. YoosefDoost & W. D. Lubitz, *Archimedes screw turbines: A sustainable development solution for green and renewable energy generation-a review of potential and design procedures*,” *Sustain.*, **12**(18), 2020, doi: 10.3390/SU12187352.
- [8] A. Hermawan, *Pilot Model Implementasi Turbin Air Jenis Kaplan Pembangkit Listrik 300 K*, Balai Besar Logam dan Mesin, Bandung, 2011.
- [9] D. S. Edirisinghe, H. S. Yang, M. S. Kim, B. H. Kim, S. P. Gunawardane, & Y. H. Lee, *Computational flow analysis on a real scale run-of-river archimedes screw turbine with a high incline angle*, *Energies*, **14**(11), pp. 1–18, 2021, doi: 10.3390/en14113307.
- [10] G. Dellinger, S. Simmons, W. D. Lubitz, P. A. Garambois, & N. Dellinger, *Effect of slope and number of blades on Archimedes screw generator power output*,” *Renew. Energy*, **136**, pp. 896–908, 2019, doi: 10.1016/j.renene.2019.01.060.
- [11] K. Shahverdi, R. Loni, B. Ghobadian, S. Gohari, S. Marofi, & E. Bellos, *Numerical Optimization Study of Archimedes Screw Turbine (AST): A case study*, *Renew. Energy*, **145**, pp. 2130–2143, 2020, doi: 10.1016/j.renene.2019.07.124.
- [12] H. B. Harja, *Kajian Eksperimental Kinerja Turbin Ulir Archimedes*, Master Thesis, Institut Teknologi Bandung, 2012.
- [13] C. Rorres, *The Turn of the Screw: Optimal Design of an Archimedes Screw*, *J. Hydraul. Eng.*, **126**(1), pp. 72–80, 2000, doi: 10.1061/(asce)0733-9429(2000)126:1(72).
- [14] D. M. Nuernbergk & C. Rorres, *Analytical Model for Water Inflow of an Archimedes Screw Used in Hydropower Generation*, *J. Hydraul. Eng.*, **139**(2), pp. 213–220, 2013, doi: 10.1061/(asce)hy.1943-7900.0000661.
- [15] G. Müller and J. Senior, *Simplified theory of Archimedean screws*,” *J. Hydraul. Res.*, **47**(5), pp. 666–669, 2009, doi: 10.3826/jhr.2009.3475.

- [16] Erinofiardi, Syaiful, M., & Prayitno, A., Electric power generation from low head simple turbine for remote area power supply, *Jurnal Teknologi (Sciences & Engineering)*, **74**(5), 21–25, 2015. <https://doi.org/10.11113/jt.v74.4636>.